International Journal of Food Microbiology 304 (2019) 39–48

Contents lists available at ScienceDirect

International Journal of Food Microbiology

journal homepage: www.elsevier.com/locate/ijfoodmicro

A novel method for rapid estimation of lactic acid bacterial concentration in fermented milk based on superhydrophobic surface wettability

Sepideh Hosseini[a], Somaye Hosseini[b], Hadi Savaloni[c,*]

[a] Department of Food Science and Technology, Pharmaceutical Sciences Branch, Islamic Azad University, Tehran, Iran
[b] Plasma Physics Research Center, Science and Research Branch, Islamic Azad University, Tehran, Iran
[c] School of Physics, College of Science, University of Tehran, Tehran, Iran

ARTICLE INFO

Keywords:
Probiotics
Microbial surface
Contact angle
Surface free energy
Hydrophobicity
Zeta potential

ABSTRACT

A novel and facile method is developed for rapid estimation of lactic acid bacterial concentration in fermented milk. Growth of bacteria in a liquid changes physicochemical property of the medium and its behavior at solid-liquid interface. Wettability determines characteristic of solid-liquid interface. Nano-rod, helical tetragonal and L-shaped morphologies were designed and fabricated. Hydrophobicity and zeta potential were measured for dried surfaces of 5 dairy bacterial strains. Relationship between microbial population and changes in solid-liquid interface was studied by wettability and surface free energy measurements. Due to hydrophobic surface property of conventional dairy strains, they strongly affect solid-liquid and liquid-vapor surface tensions when dispersed in a liquid, which are dependent on the bacterial concentration. Response surface methodology results showed that type and concentration of bacteria, droplet volume and solid–surface morphology affect wettability significantly. Higher hydrophobicity resulted in higher $\Delta\theta$ (absolute value of the difference between the pure physiological saline and the bacterial suspension contact angles) dependence on the bacterial concentration. Probiotic bacteria concentration in fermented milk was estimated using the proposed method. A direct relationship was obtained between milk contact angle and bacterial concentration. Results show that this physical method can be applied for rapid estimation of bacterial concentration.

1. Introduction

Identification, control, and development of microorganisms are the major concerns in food manufacture especially in various fermented and probiotic food products (Fernandes et al., 2014). Despite the increase in the importance of microorganisms in food science, new rapid estimation methods for determining their population has been less studied. Most of the related studies are mainly focused on the chemical, biochemical, or spectrophotometry methods. In the biochemical methods, biosensors or pure antibodies are required to estimate the concentration of microorganisms, which could be expensive and time-consuming (at least 4 to 72 h) (Mazumdara et al., 2007). On the other hand, physical methods such as spectrophotometry and fluorescence microscopy that may rapidly estimate the number of bacteria in milk and other liquid foods, have other problems such as depending on a specific complex device/apparatus and interfering food components (proteins and lipids) (Välimaa et al., 2015).

The chemical composition and physicochemical properties of a cell surface are the basis of the methods for estimating their population, adhesion, or distribution in different media (Bohinc et al., 2016). Hydrophobicity, surface-free energy, and electric charge are the most important physical properties of a microbial surface (Pelletier et al., 1997). Although these properties have been identified for most commercial strains, their application has received less attention so far. Microbial surface properties are typically assessed to determine their adhesion to different surfaces (Deepika and Charalampopoulos, 2010). Results showed that microbial adhesion to different food-contact surfaces or the gut wall strongly depends on the cell surface hydrophobicity and substrate morphology (Pretzer et al., 2005). Probiotic strains, especially lactic acid bacteria, have a hydrophobic surface. This characteristic is strongly associated with the carbon-to-nitrogen ratio of the surface. By reducing their nitrogen on the surface, their hydrophobicity increases (Frece et al., 2005). Considering that the surface of most microorganisms is hydrophobic, their growth in a liquid medium should increase the hydrophobicity property (Di Ciccio et al., 2015). This results in a change in the surface tension of the medium, which in turn changes the behavior of the solid-liquid, and solid-vapor interfaces. Liquid surface tension is the main parameter in droplet shape and

* Corresponding author.
E-mail address: savaloni@khayam.ut.ac.ir (H. Savaloni).

https://doi.org/10.1016/j.ijfoodmicro.2019.05.015
Received 6 May 2018; Received in revised form 14 May 2019; Accepted 20 May 2019
Available online 25 May 2019

their contact angle (Young, 1805).

The aim of this study is to evaluate the effect of increasing the bacterial population in the liquid medium on changing the shape of the droplet and consequently its contact angle on the solid surface. For this purpose, surface properties of five bacterial strains commonly used in the dairy industry (*Streptococcus thermophilus*, *Lactobacillus bulgaricus*, *Lactobacillus acidophilus*, *Lactobacillus casei*, *and Lactobacillus plantarum*) were determined and the contact angle of liquid droplets of different concentrations of these bacteria on different nano-sculptured solid surfaces, namely nano-rod, helical tetragonal and L-shaped structures was measured. In addition, the influence of the type of strain, bacterial concentration, size of droplet, and solid surface morphology on the contact angle of liquid droplet on solid surface was studied by measuring the response surface methodology (RSM) as the experimental design. Finally, to evaluate the applicability of this method, changes in the contact angle of milk droplet during fermentation by *L. casei* and *L. pantarum* were investigated, and the results were used to estimate the milk bacterial population.

2. Materials and methods

2.1. Bacterial strain, growth conditions and enumeration

The microorganisms used in this study were *Streptococcus salivarius* subsp. *thermophilus* DSM 20617, *Lactobacillus delbrueckii* subsp. *bulgaricus* DSM 20081, *Lactobacillus acidophilus* DSM 20079, *Lactobacillus casei* ATCC 39392, and *Lactobacillus plantarum* DSM 20205. The cultures were provided in the freeze-dried form, and the storage and maintenance of the cultures were carried out according to the manufacturer's recommendation.

The microorganisms were activated and pre-cultured under appropriate conditions given in Table 1. Next, the cells were harvested by centrifugation at 4 °C for 15 min (10,000 ×*g*), then the precipitated cells were washed twice with sterile physiological saline and re-suspended in 10 mL of physiological saline.

Bacterial enumeration was performed by serial dilution in the ringer's solution and then pour plating in the related medium using petri plates. The plates were incubated at appropriate condition (72 h at 37 °C), with subsequent quantification of bacteria and results being expressed as colony-forming log unit (CFU) per mL of original samples (Tharmaraj and Shah, 2003). The average of three enumerations was accepted as the result given in the following sections.

2.2. The surface physical properties of bacteria

Cell surface hydrophobicity was determined by measuring the contact angle (θ_w) between a water droplet (size: 10 mg) and the dried flat layer of bacteria according to the method described by Boonaert and Rouxhet (Boonaert and Rouxhet, 2000). Bacterial suspensions were filtered under reduced pressure onto a mixed cellulose esters filter (47 mm diameter, pore size 0.45 μm, HAWP, Millipore Co., Bedford, Mass). In order to achieve the constant moisture content, the filter with bacteria was transferred into 1% agar (w/v) in water containing 10% (v/v) glycerol for 3 min. Then, the filters were fixed on a microscope slide and dried at 37 °C for 3 h (Reid et al., 1992).

Zeta potential (ζ), Electrophoretic mobility is determined based on migration time of cells under the constant electric field. For this purpose, microbial suspensions (concentration about 3×10^8 per mL) in 1 mM of KNO_3 at different pH were prepared and then the zeta potential of the cell surface was assessed by zeta-sizer (Malvern-Zen3600, UK) (Tymczyszyn et al., 2008).

2.3. Milk fermentation

Fat free (< 0.05%) ultra-high temperature (UHT) milk was purchased from Mihan Co. Tehran, Iran. The milk was transferred under aseptic conditions to 100 mL containers and inoculated with 2% (v/v) each of *L. casei* and *L. plantarum*.

The inoculated milk was incubated at 32 °C for 24 h, viable bacterial enumeration and the contact angle measurements between milk and superhydrophobic (rose-petal effect) surface was carried out at defined intervals (Shobharani and Agrawal, 2010).

Pour-plate technique was applied to count the milk probiotic bacteria (Macciola et al., 2008). 2 mL of fermented milk sample was diluted in 18 mL of quarter strength of the Ringer's solution. Next, in order to obtain appropriate bacterial concentrations (10^2–10^6 mL^{-1}) serial dilution process was carried out. 100 μL of different dilutions were inoculated on the MRS Agar culture medium and incubated for 72 h at 37 °C. Plates containing 25 to 250 colonies were selected, and the results of counting were reported as $\log_{10}$ of the colony-forming unit per mL of fermented milk.

2.4. Fabrication of metal solid surfaces

Nano-sculptured manganese thin films with different shapes and morphologies were deposited on glass (microscope slides) substrates by electron beam evaporation from a graphite crucible of 6 mm diameter at room temperature with the constant deposition rate of 1.0 $Å s^{-1}$. For this purpose, an Edwards (Edwards E19 A3) coating plant with a base pressure of 2×10^{-7} mbar was used.

Two stepping motors that can rotate the substrate holder by the two angles α and φ, with 0.01°/step accuracy and controlled speed, control the substrate holder system. The movement of the stepper motor for rotation of substrates about its surface normal (φ) and its speed of

Table 1
Growth condition and the physical characterization of microorganisms' surfaces.

Microorganisms	Strain	Medium	Cultivation conditions	Zeta potential (mV)*			Contact angle(°)**
				pH = 2	pH = 7	pI	θ_w
S. thermophilus	DSM 20617	Trypticase Soy Yeast Extract	45 °C, microaerophilic	1.3 ± 0.6^a	−21.3 ± 2.2^a	2.6 ± 0.7^a	33 ± 4^a
L. bulgaricus	DSM 20081	MRS Broth	37 °C, anaerobic	−14.2 ± 1.4^d	−36.5 ± 3.1^c	ND	122 ± 6^d
L. acidophilus	DSM 20079	MRS Broth with 0.05% cysteine-hydrochloride	37 °C, anaerobic	−7.1 ± 2.5^b	−41.5 ± 2.7^d	ND	117 ± 5^{cd}
L. casei	ATCC 39392	MRS Broth	30 °C, aerobic	9.1 ± 0.9^c	−29.6 ± 1.2^b	4.2 ± 1.1^b	71 ± 7^b
L. plantarum	DSM 20205	MRS Broth	30 °C, aerobic	−7.2 ± 1.4^b	−40.4 ± 2.3^{d,c}	ND	109 ± 4^c

Different superscript letters (a, b, c) in the same column mean significant differences ($p \leq 0.05$).

* The zeta potential values are means of 3 to 5 measurements.

** The hydrophobicity values are means of three measurements.

revolution, along with the facility for dividing each revolution to different sectors, were controlled through the interface to a computer in which the related software (in the LABVIEW format) is written and installed. All these were made domestically.

Nano-rod samples (500 nm in thickness) were deposited at the surface normal deposition angle, while the helical tetragonal and L-shaped sculptured thin films were deposited at 83° and 80° deposition angles, respectively. The helical tetragonal structures was fabricated with 100 nm arm length at a fixed α angle, then the substrate holder was rotated by 90° until the second arm of the same length was formed. The rotation of the substrate with this angle was continued to obtain the helical sculptured structure with 330 nm thickness consisting of four pitches.

The L-shaped sample was formed by rotation of substrate holder clockwise about its normal surface with different speeds at different stages. At the first stage, the substrate holder was rotated at a speed of 0.03 rpm for 2000 s to produce a pitch with a diameter of 164 nm and thickness of 25 nm. Then, the substrate rotation speed was increased to 0.3 rpm for 1000 s to establish five smaller diameters (50 nm) pitches with a thickness of 160 nm. At the final stage, the substrate holder was fixed and the deposition was continued until a nano-rod with a length of 300 nm was fabricated. The film thicknesses as well as column shapes and sizes were measured using a field emission electron microscope (FESEM) (Hitachi S-4100 SEM, Japan). The FESEM samples were coated with a very thin layer of gold to prevent the charging effect. Physical morphology and roughness were obtained by means of the AFM (Park scientific instruments model Autoprobe) analysis with a Si tip of 10 nm in diameter and in non-contact mode.

2.5. Measurement of the contact angle

Measurement of the static, advancing, receding and the hysteresis of contact angles of the water droplet with the solid surface was carried out using a domestic made instrument with a 5-dioptre lens and digital camera (model DCR-SR200E, Sony, Japan). The advancing and receding contact angles were measured by releasing a droplet of 10 mg on the substrate surface and by pumping in and out of a further 30 mg of liquid in this droplet, respectively. The hysteresis of the contact angle was obtained as the difference between advancing and receding contact angles. The analysis of the contact angle was performed by ImageJ software code and the method of Low Bond Axisymmetric Drop Shape Analysis (LB-ADSA) which is designed by (Stalder et al., 2006) and used in the Young–Laplace analysis (Stalder et al., 2006; Hosseini et al., 2017). This code uses the droplet image on the solid surface and measures the contact angle by precision of two digits. The average of contact angles of several droplets on reproduced samples was used to obtain the contact angle and calculate the uncertainty of the data. Then these values were rounded to one digit in Table 2.

The size of the contact angle is used to classify solid surfaces, namely hydrophilic ($\theta < 90°$), hydrophobic ($90° < \theta < 150°$), and superhydrophobic ($150° < \theta < 180°$) (Gao et al., 2009).

2.6. Surface free energy

The surface free energy can be calculated by the Young's equation:

$$\gamma_{sv} = \gamma_{sl} + \gamma_{lv}\cos\theta_Y \quad (1)$$

where θ_Y is the Young contact angle between the liquid and the solid surface and γ_{lv} and γ_{sl} are liquid-vapor and solid-liquid tensions, respectively. In this equation γ_{sl} cannot be measured directly, hence calculation of γ_{sv} is subject to some complications. γ_{sv} of different solid -vapor were calculated by the acid-base method (which is also known as the Van Oss-Chaudhry-Good method) (Hosseini et al., 2017; Van Oss et al., 1986; Van Oss, 2006).

γ_{lv} of bacterial suspension was calculated according to the Neumann method (Kwok and Neumann, 1999):

$$\cos\theta_Y = -1 + 2\sqrt{\frac{\gamma_{sv}}{\gamma_{lv}}}\,e^{-\beta(\gamma_{lv}-\gamma_{sv})^2} \quad (2)$$

The coefficient $\beta = 0.0013$ was determined by using the value of $\gamma_{lv} = 72.8\ \mathrm{mJm^{-2}}$ for water as reported by Van Oss et al. (1986) and $\gamma_{sv} = 110.9\ \mathrm{mJm^{-2}}$ calculated by Hosseini et al. (2017).

These values were calculated by acid-base method when $\theta_Y = 129.1°$ is for 10 mg water droplet.

2.7. Statistical procedures

Response surface methodology (RSM) and the optimal design were used to study the effects of the independent variables: bacterial strains (X1), bacterial population (X2), droplet size (X3), and solid substrate (X4) on the dependent variable: changes of the contact angle between solid and liquid. The RSM data analyses were performed using Design expert 10 (Stat-Ease, USA).

The analysis of variance (ANOVA) was used to predict the significance of the changes in the contact angle ($P < 0.05$; P is the probability value) with bacteria concentration (Fig. 3). In addition, Duncan analyses (IBM SPSS 23, Boston College) was performed for achieving more refined analysis of the ANOVA results distinguishing the variation of contact angle with bacteria concentration in for even smaller changes in bacteria concentration.

Key Resources Table

Resource	Source	Identifier
Chemical		
Esters		
Format		
Glycerol		
Gold		
KNO3		
Manganese		
Ringer's solution		

3. Results and discussion

3.1. Surface physical properties of bacteria

Table 1 shows the surface physical properties of five different bacterial species examined in this work, namely *S. thermophilus*, *L. bulgaricus*, *L. acidophilus*, *L. casei* and *L. plantarum*. All the bacteria samples

Table 2
Structural characteristics of different Mn sculptured thin films produced in this work (results are given as means ± SD).

Morphology	Number of arms	Film Thickness (nm)	R_{avg} (nm)	R_{rms} (nm)	F_v (%)	ϑ (°)	θ_{Ad} (°)	θ_{Rd} (°)	CAH (°)
Nano-rod	1	500	1.4 ± 0.8[a]	1.8 ± 0.2[a]	12.2 ± 2.0[a]	51.2 ± 0.4[a]	54.4 ± 1.9[a]	18.5 ± 2.3[a]	35.9
L-shaped	3	450	80.9 ± 1.8[b]	83.3 ± 1.6[c]	84.2 ± 2.7[b]	129.1 ± 1.1[b]	141.8 ± 2.0[b]	47.5 ± 1.8[b]	94.3
Tetragonal	16	330	58.3 ± 2.2[c]	62.4 ± 1.9[b]	89.2 ± 4.4[b]	151.5 ± 0.7[c]	160.4 ± 2.3[c]	53.6 ± 0.5[c]	106.8

a, b, and c) indicate the significant difference between different parameters (Duncan, $P < 0.05$). F_v) surface void fraction; ϑ) static contact angle; θ_{Ad})) advancing contact angle; θ_{Rd}) receding contact angle; CAH) hysteresis contact angle.

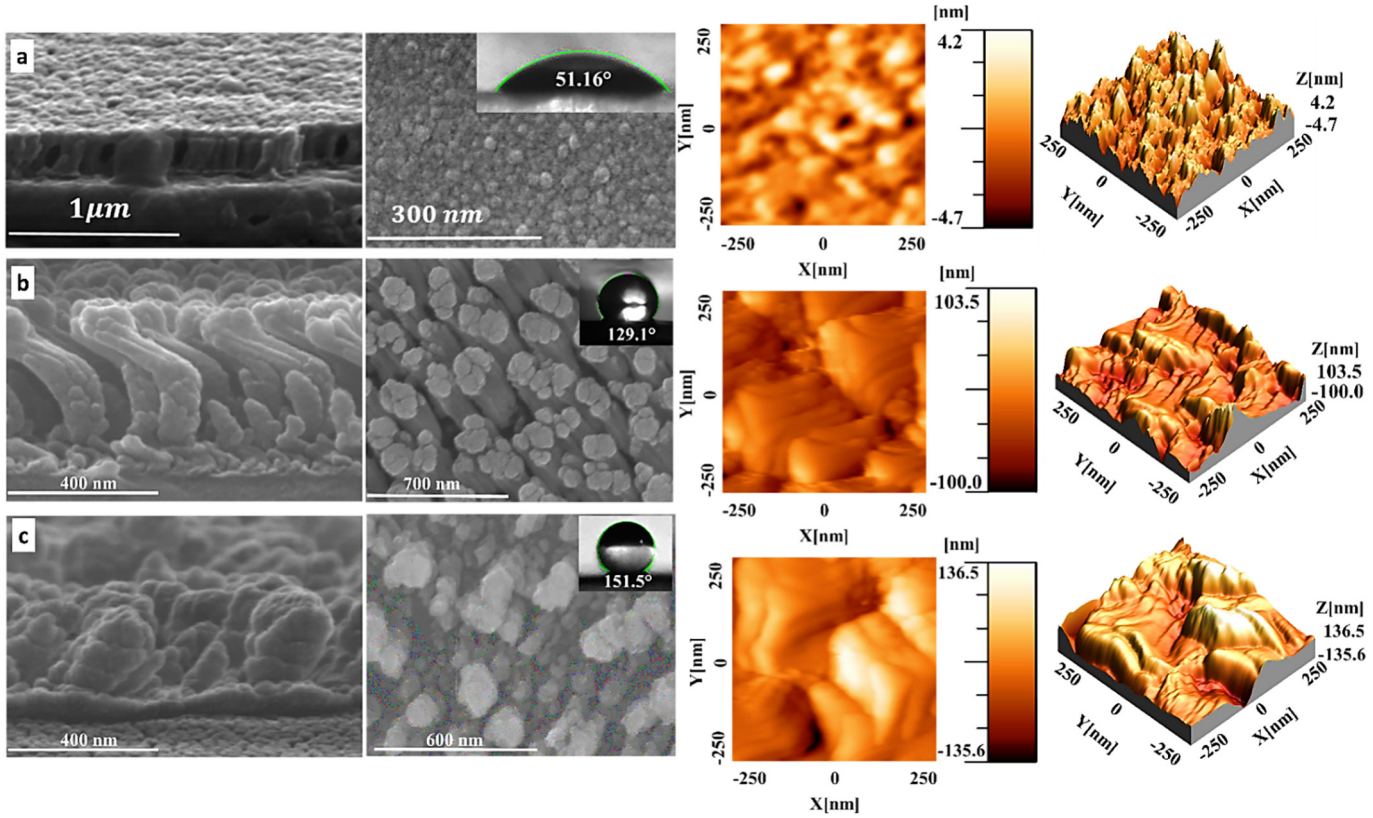

Fig. 1. Cross-section and surface FESEM images and 2D and 3D AFM images of (a) 500 nm Mn nano-rod thin film deposited at normal angle to the substrate surface without rotation of substrate holder (b) L-shaped sculptured Mn thin films with rotation of substrate holder (c) helical tetragonal sculptured Mn thin film deposited at 83° with 16 arms (see text for details of depositions). The contact angle for water droplet (inset of (FESEM image)).

show negative zeta potential at pH = 7. Zeta potential of all bacterial surfaces shifted towards positive values by reducing the pH. The isoelectric point (pI) of *S. thermophilus* and *L. casei* are 2.6 and 4.2, respectively (Table 1: a, b, c, and d letters are used to show different contact angles and/or zeta potential, respectively with significant difference ($P < 0.05$)), while other species are negatively charged at all pH values (e.g., 2–7) and no isoelectric point was observed. Zeta potential is the potential difference between dispersed bacterial surface and the dispersing liquid medium that can be assumed as surface charge density. Considering that all bacteria indicate a high negative magnitude for zeta potential in pH = 7 (> 20 mV, Table 1 column 6), there is a very low possibility of flocculation or agglomeration in bacterial suspension. Hence, it can be concluded that bacterial suspension at pH close to 7 has uniform distribution, which is the necessary condition for the sampling process in the following section.

Results of the contact angles between water droplet and the different dried bacterial surfaces are given in Table 1 column 8. As can be seen, the hydrophobicity of bacterial surface varies significantly for different species. *L. bulgaricus* and *S. thermophilus* show high hydrophobic and hydrophilic surfaces, respectively. It should be noted that the contact angle reported by this method is not necessarily very reliable because the contact angle of bacterial surfaces can be affected by the drying method, temperature, and serial culture passages (Reid et al., 1992; Tymczyszyn et al., 2008). *S. thermophilus* and *L. casei*, which have isoelectric points of 2.6 and 4.2 also show hydrophilic surfaces (Table 1, column 8).

There has been no conclusive study on the relationship between bacterial cell surface charge and wetting properties, but most studies have shown that the presence of glyco-proteinaceous material in the cell surface increases hydrophobicity, while surface hydrophilicity is dependent on the presence of polysaccharides (Cuperus et al., 1993; Mozes et al., 1991). The outer surface of species with an isoelectric point in the range from about 2 to 4 often contains carboxyl and/or phosphorylated sugar units, which often are hydrophilic and cause the outer surface to be partially hydrophilic (Rijnaarts et al., 1995). Hydrophobicity of cells are also related to Van der Waals, electrostatic forces and Lewis acid-base interactions. Bellon-Fontaine et al. (1996) did not obtain electrophoretic mobility in cell surfaces at isoelectric pH even though there still was cell hydrophobicity and concluded that electrostatic interactions have little effect on cell hydrophobicity in this condition. In this study, the examined contact angles were measured at pH = 7. Hence, it may be suggested that all three forces mentioned above could effectively affect the results.

3.2. The surface physical properties of metal thin films

Three different Mn nano-sculptured thin films with different morphologies and geometries, namely nano-rod, helical tetragonal and L-shaped were fabricated as described in Section 2.7.

In Fig. 1 FESEM images of the surface, cross-section and the 2D and 3D AFM images of the above mentioned samples are shown. AFM images were analysed by Spip code, and the roughness and void fraction of surfaces were calculated by considering grains on the 2D image of each structure. Structural characteristics of these thin films are given in Table 2 (a, b and c letters in Table 2 are used to show different surface roughness, void fraction and contact angles with significant difference ($P < 0.05$)).

The influence of surface roughness and void fraction on the contact angle are well reported in the published literature (Yang et al., 2006; Stanton et al., 2012). In an earlier work (Hosseini et al., 2017), thoroughly investigated and discussed the effect of these parameters as well as surface symmetry on super/hydrophobicity/hydrophilicity on different metal surfaces (nano-rod, helical pentagon and helical tetragonal). They showed that by using different structural geometries, the

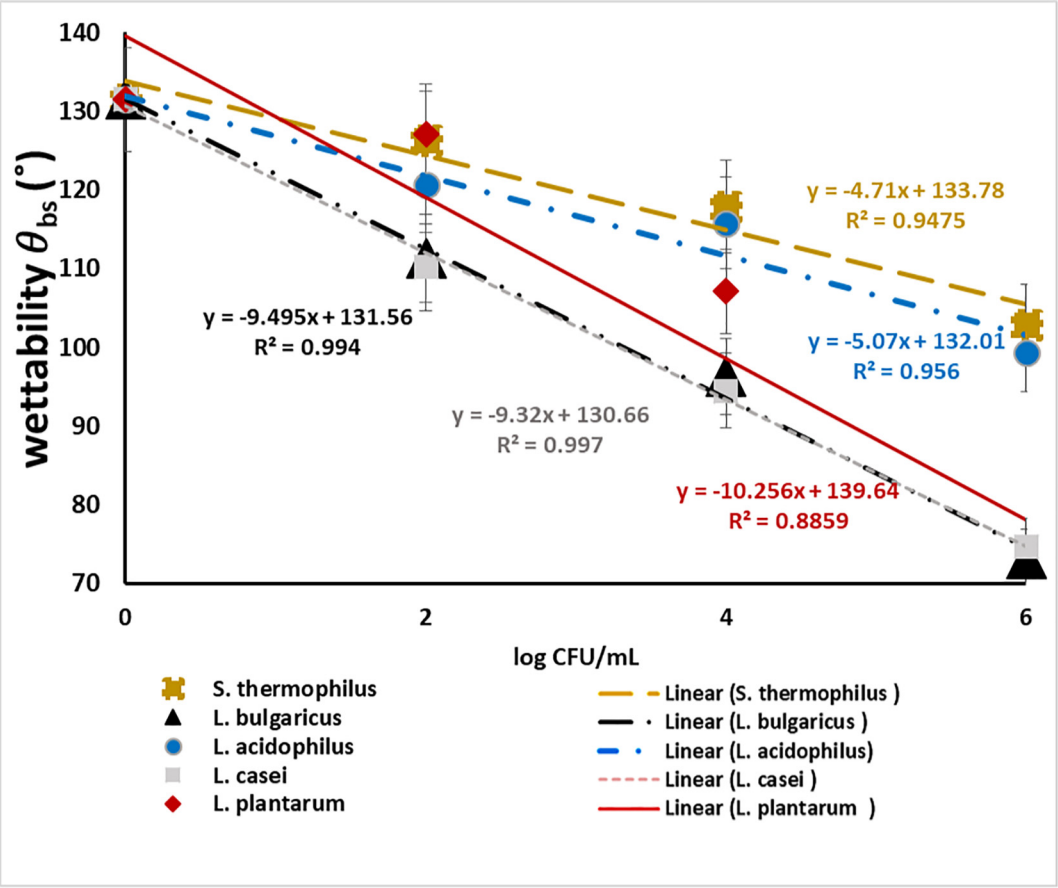

Fig. 2. Wettability of L-shaped structure for different bacterial species with different concentrations.

Table 3
Wettability of L-shaped structure for different bacterial species with different concentrations and Pearson correlation coefficient.

Bacteria	Wettability				Pearson correlation coefficient
	0 log CFU/mL	2 log CFU/mL	4 log CFU/mL	6 log CFU/mL	
S. thermophilus	131.5 ± 0.6^{d}	126.3 ± 1.8^{c*}	117.9 ± 1.2^{b}	102.9 ± 1.6^{a}	−0.9734
L. bulgaricus	131.5 ± 0.6^{d}	111.3 ± 0.5^{c}	96.3 ± 0.7^{b}	73.2 ± 1.1^{a}	−0.9962
L. acidophilus	131.5 ± 0.6^{d}	120.6 ± 1.3^{c}	115.8 ± 1.8^{b}	99.3 ± 0.9^{a}	−0.9777
L. casei	131.5 ± 0.6^{d}	110.2 ± 0.6^{c}	94.5 ± 0.8^{b}	74.6 ± 1.4^{a}	−0.9984
L. plantarum	131.5 ± 0.6^{d}	127.1 ± 1.2^{c*}	107.1 ± 1.5^{b}	69.8 ± 0.5^{a}	−0.9412

a, b, c and d) indicate the significant decrease of contact angle with bacteria concentration, respectively (Duncan, $P < 0.05$).
* Significant difference in paired bacterial species was obtained for all bacteria but those shown with (*) ($P > 0.05$).

hydrophobicity could be tuned from low hydrophobic to super-hydrophobic. Result of their work also showed that a higher degree of hydrophobicity can be achieved from a higher void fraction and increased surface roughness. Influences of different parameters (i.e., growth angle, void fraction, structural symmetry and volume of water drop) on the hydrophobic property were investigated. Results showed that hydrophobicity increases with the surface roughness, structural order and void fraction.

The wettability verification of solid surfaces was determined by smoothly releasing 10 mg of distilled water droplets on them. The values of contact angle are illustrated in Fig. 1 and Table 2. According to the results, the surfaces were classified as superhydrophobic (θ = 151.5°), hydrophobic (θ = 129.1°), and hydrophilic (θ = 51.2°) for helical tetragonal, L-shaped, and nano-rod structures, respectively.

In Table 2 detailed characteristics of the structural analyses including surface roughness, void fraction, contact angle hysteresis (CAH) and statistical analyses are given. All results show that contact angle and CAH increase with void fraction while when the surface roughness is decreased in case of helical tetragonal structure relative to the L-shaped structure opposite result is obtained. In this case the statistical analyses show similar results which can be due to either competition of void fraction with surface roughness or the complexity of the tetragonal structure when compared with simple structure of the L-shaped film.

3.3. Solid surface wettability by microbial suspension

The influence of bacterial population in a liquid and changes in the interfacial characteristics were investigated by the wettability method. Results of the contact angle between various concentrations of different bacteria in physiological saline and hydrophobic surface (L-shaped structure) are given in Fig. 2 and Table 3. Statistical analyses of the experimental data were carried out using ANOVA and Duncan tests, which are summarized in Fig. 2 (as an indication of correlation between contact angle and the bacteria concentration) and Table 3. In addition,

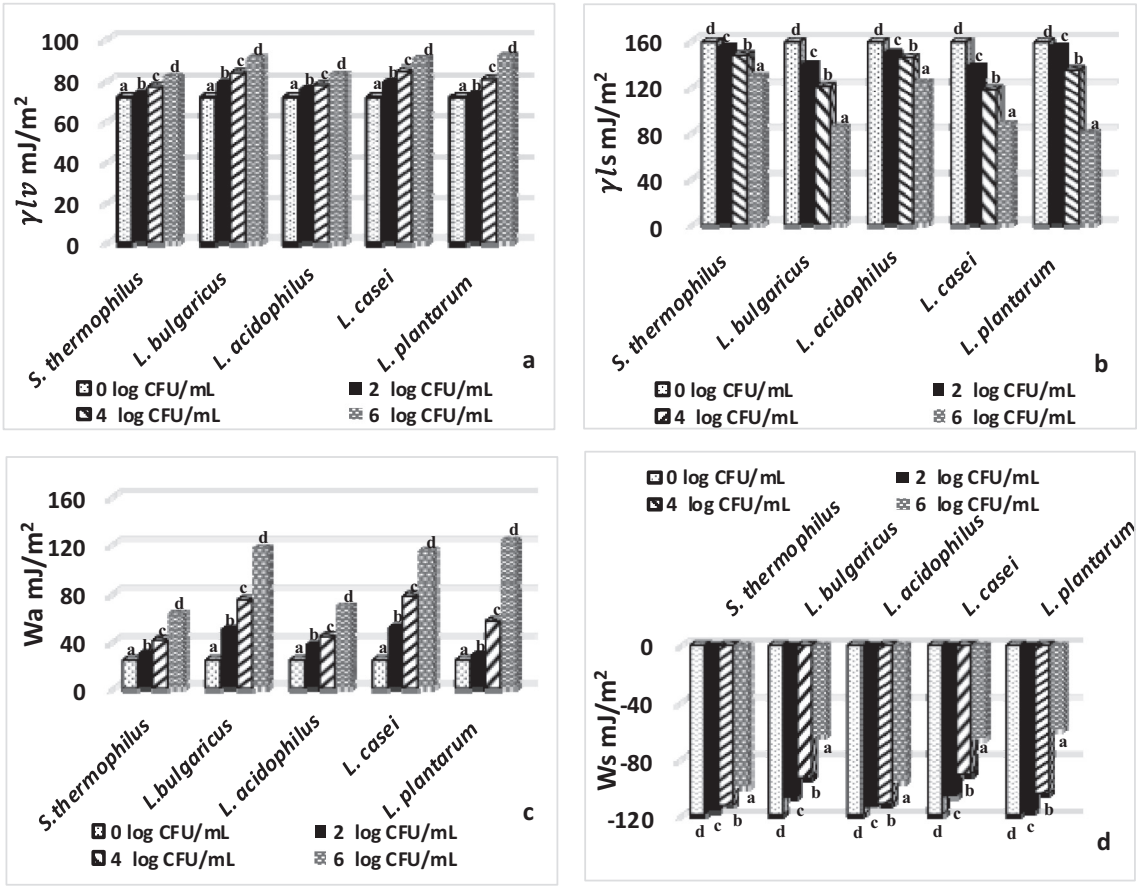

Fig. 3. Surface free energy of droplet containing different species with different concentrations in contact with L-shaped structure; (a) liquid-vapor tensions values calculated from Newman equation, (b) values of solid-liquid tensions calculated from Young equation, (c) Work of adhesion, (d) Work of spreading. a, b, c and d) indicate the significant difference of different parameters with bacteria concentration, respectively (Duncan, $P < 0.05$).

results obtained from ANOVA shows that the type of bacteria also influences the contact angle. The only overlapping/same data ($P > 0.05$) is for *S. themophilus and L. plantarum* bacteria when two bacteria concentration is log 2 CFU/mL. The contact angle of blank samples containing no bacteria is 131.5 ± 0.6° which reduces significantly ($P < 0.05$) with increasing the bacterial concentration (Table 3). This confirms that bacterial growth changes the contact angle of the droplet. In Fig. 3 it can also be seen that the contact angle decreases linearly with bacteria concentration and the slope of this linear reduction can be classified in two groups as; a) *L. plantarum*, *L Casei* and *L. bulgaricus* with high slope (~−9.5), and b) *S. themophilus* and *L. acidophilus* with low slope (~−4.9). However, if these results (group of two sets of bacteria) are compared with those contact angles obtained for bacteria hydrophobicity in Table 1 it can be seen that there is no correlation between contact angle reduction and bacteria hydrophobicity. Hence, it can be concluded that the method may be used irrespective of the wetting property of bacteria film.

Various parameters such as bacterial growth phase and ingredient of the medium, may affect the bacterial outer surface and consequently the contact angle. In addition, solid surface properties and surface free energy significantly change the contact angle (Bohinc et al., 2016); therefore, the value of contact angle could not exactly specify bacterial strain or concentrations without considering experimental conditions, but its changes may be applied as a fast and purely a physical method to estimate bacterial concentrations. In the following sections, we develop foundations for the use of this change in the contact angle to estimate lactic acid bacterial concentration.

3.4. The effect of microbial growth on surface free energy

Further analyses were carried out using ANOVA and Duncan methods on surface free energy, work of adhesion and work of spreading. In Fig. 3, a, b, c, and d letters are used to show different contact angles with significant difference ($P < 0.05$).

Liquid-vapor (γ_{lv}) and solid-liquid (γ_{ls}) tensions for different bacterial concentration were calculated by releasing 10 mg of bacterial suspension on L-shaped thin films and applying Young and Newman equations (Eqs. (1) and (2), respectively). Results of γ_{lv} showed that liquid-vapor tension increases with bacterial concentration (Fig. 3a). Considering that work of cohesion W_c is related to γ_{lv} ($W_c = 2\ \gamma_{lv}$), it can be assumed that cohesion of bacterial suspensions also can increase with bacterial concentration. Furthermore, solid-liquid (γ_{ls}) tension between bacterial suspension and L-shaped surface reduced by increasing bacterial concentration (Fig. 3b). These could be the reasons for the change in the droplet shape when in contact with the solid surfaces. The work of adhesion is the energy, which was released in the process of wetting and may be calculated as:

$$W_a = \gamma_{lv}(\cos\theta + 1) \quad (3)$$

It can be observed that W_a increases with bacterial concentration in the droplet (Fig. 3c). Wettability of solid surface may be identified by the adhesive work (W_a) while spreading work (W_S) also confirms this property (Fig. 3d).

3.5. Effective variables on the contact angle of bacterial suspension

The results of Section 3.3 showed that the species of bacteria and

Table 4
Scheme of optimal design: independent (X) and response variables (Y).

Run	X1	X2	X3	X4	Y1
	Numbers of bacteria (CFU/mL)	Droplet size (mg)	Strain	Shape	Δθ(°)
1	5	30	*L. casei*	Tetragonal	88.1
2	7	90	*L. acidophilus*	Nano-rod	15.4
3	4	53	*L. bulgaricus*	L-shaped	29.8
4	3	10	*S. thermophilus*	Tetragonal	31.4
5	8	16	*L. bulgaricus*	L-shaped	60.9
6	6	37	*L. acidophilus*	L-shaped	39.3
7	9	67	*S. thermophilus*	L-shaped	35.7
8	4	20	*L. acidophilus*	L-shaped	19.2
9	8	16	*L. bulgaricus*	L-shaped	41.7
10	9	10	*L. casei*	Nano-rod	14.0
11	7	62	*L. acidophilus*	Nano-rod	11.5
12	2	64	*L. plantarum*	L-shaped	19.1
13	3	66	*L. bulgaricus*	Tetragonal	69.2
14	3	46	*L. casei*	Tetragonal	71.6
15	3	55	*L. plantarum*	Nano-rod	2.7
16	4	63	*L. bulgaricus*	Tetragonal	69.5
17	5	48	*S. thermophilus*	Nano-rod	2.0
18	7	52	*L. bulgaricus*	Nano-rod	17.2
19	9	30	*S. thermophilus*	Nano-rod	5.9
20	1	30	*L. bulgaricus*	Nano-rod	0.5
21	7	67	*L. casei*	Nano-rod	12.9
22	3	50	*L. acidophilus*	Tetragonal	39.3
23	4	11	*S. thermophilus*	Tetragonal	35.2
24	5	54	*S. thermophilus*	Nano-rod	2.3
25	3	10	*L. casei*	Nano-rod	5.6
26	5	50	*L. plantarum*	Tetragonal	57.4
27	9	65	*L. casei*	L-shaped	50.8
28	1	10	*S. thermophilus*	L-shaped	40.1
29	9	37	*L. plantarum*	L-shaped	48.8
30	7	10	*L. plantarum*	Nano-rod	9.5
31	8	90	*L. acidophilus*	Nano-rod	16.8
32	4	50	*L. casei*	L-shaped	30.2
33	2	64	*L. plantarum*	L-shaped	25.9
34	1	90	*L. acidophilus*	Nano-rod	7.4
35	3	37	*S. thermophilus*	L-shaped	23.6
36	3	46	*L. casei*	Tetragonal	43.3
37	3	37	*S. thermophilus*	L-shaped	29.8
38	4	52	*L. plantarum*	Tetragonal	43.3
39	5	51	*L. bulgaricus*	Nano-rod	16.0
40	6	88	*L. acidophilus*	Tetragonal	71.9
41	6	88	*L. acidophilus*	Tetragonal	73.7

Table 5
Analysis of variance (ANOVA) of experimental results for (Δθ).

Dependent variables	Independent variables	Sum of squares	F-value	*P*-value
Δθ	Log numbers of bacteria (CFU/mL)	13.24	20.56	< 0.0003
	Droplet size (mg)	0.83	1.30	0.2296
	Strain	7.14	3.06	0.0253
	Shape of substrate	175.70	137.70	< 0.0001
	Droplet size × shape	3.88	3.50	0.0427
	Lack of fit	14.06	0.54	0.87
	Pure error	3.12	–	–
	Cor total	209.61	–	–

their population in droplets influence the contact angle of bacterial suspension. Earlier studies (Kwon et al., 2011; Murakami et al., 2014) reported that the size of liquid droplet and solid surface morphology affect the contact angle.

The RSM was used to study the effect of four independent variables: bacterial concentration (1–9 log CFU/mL), five different species of Lactic acid bacteria, the size of the suspension droplet (10 to 90 mg), three different substrate morphologies (nano-rod (hydrophilic), L-shaped (hydrophobic) and helical tetragonal (superhydrophobic) on the contact angle. It is important to note that the absolute value of the difference between the pure physiological saline contact angle and the bacterial suspension contact angle is considered as the dependent variable ($\Delta\theta$). Hereafter is called absolute angle. The experimental data of the studied variables are presented in Table 4. The RSM analysis showed that the quadratic polynomial response model produces the highest coefficient value ($R^2 = 0.9701$) to predict the absolute angle (Δθ) values. This shows that this model adequately describes > 90% of the influence of independent variables on changes of the contact angle.

The analysis of variance (ANOVA) of results shows that the substrate morphology and the population of bacteria and strains have significant ($P < 0.05$) influence on the absolute angle (Δθ) (Table 5). However, the linear term of droplet size showed a non-significant ($P > 0.05$) effect, and, furthermore, the interaction terms of substrate morphology and droplet size was found to have a significant effect ($P < 0.05$) on the absolute angle (Δθ) (Table 5).

The absolute angle (Δθ) increased significantly ($P < 0.05$) with concentrations of all studied strains in the suspension (Fig. 4). *L. plantarum* (Fig. 4d) and *S. thermophilus* (Fig. 4b) exhibited the highest and lowest changes, respectively.

Surface wettability can be attributed to the competition between cohesion in liquid-liquid phase versus adhesion in liquid-solid phase, which was described in preceding section. Van der Waals force could increase adhesion between substrates (solid phases) and droplet. As shown in Table 1, all the bacteria studied in this work have negative zeta potential. As mentioned before, the zeta potential could assume as the surface charge density (Neu, 1996) and so it can be said that by increasing the bacterial concentration, electrostatic and Van der Waals attractive forces may also increase. Hence, the work of adhesion increases with bacterial concentration (Fig. 3c) which leads to increase of the absolute angle (Δθ) (Fig. 4). Comparison of sub-figures in Fig. 4 shows that the absolute angle (Δθ) for *S. thermophiles* for small droplet sizes is less than other bacteria used in this work. This could be due to the fact that these bacteria have the lowest surface charge density in pH = 7 which leads to weaker electrostatic interactions.

In Fig. 5(a–c), the influence of substrate morphology (i.e. helical tetragonal, L-shaped, and nano-rod) on absolute angle (Δθ) for different droplet sizes and different concentration of bacteria (*L. casei*) is exhibited. The strongest dependence on both bacterial concentration and the droplet size is obtained for the helical tetragonal structure (Fig. 5a). The hydrophilic nano-rod structure showed very slight variation of contact angle for different concentrations of bacteria (Fig. 5c).

It is reported (Hosseini et al., 2017) that surface roughness, void fraction, and symmetry of the surface are the most important parameters, which influence the hydrophobicity of the surface. In Table 2, average surface roughness, the root mean square surface roughness, and the surface void fraction are given. If the data given in Fig. 4 and Table 2 for the nano-rod structure is compared with other structures (e.g., helical tetragonal and L-shaped), it can be seen that the surface roughness and the void fraction have a significant effect on absolute angle (Δθ) under the same condition of bacterial concentration and droplet size. As can be seen, helical tetragonal and L-shaped structures have almost identical roughness and void fraction, while the nano-rod structure has the lowest surface roughness and lowest surface void fraction (Table 2, Columns 2 and 3). Generally, superhydrophobic (rose-petal effect) surface when compared with hydrophobic and hydrophilic solid surfaces showed the high ability for identifying the relationship between contact angle and bacterial population (Fig. 1).

As shown in Fig. 5 absolute angle (Δθ) depends on both droplet size and the surface morphology of solid substrate. This is more pronounced for the helical tetragonal surface. This surface shows that for different concentrations of bacteria and droplet sizes (apart from droplet sizes between 40 and 60 mg), a reasonable change occurs in the value of Δθ, which may be used as application of this method for determination of bacterial concentrations.

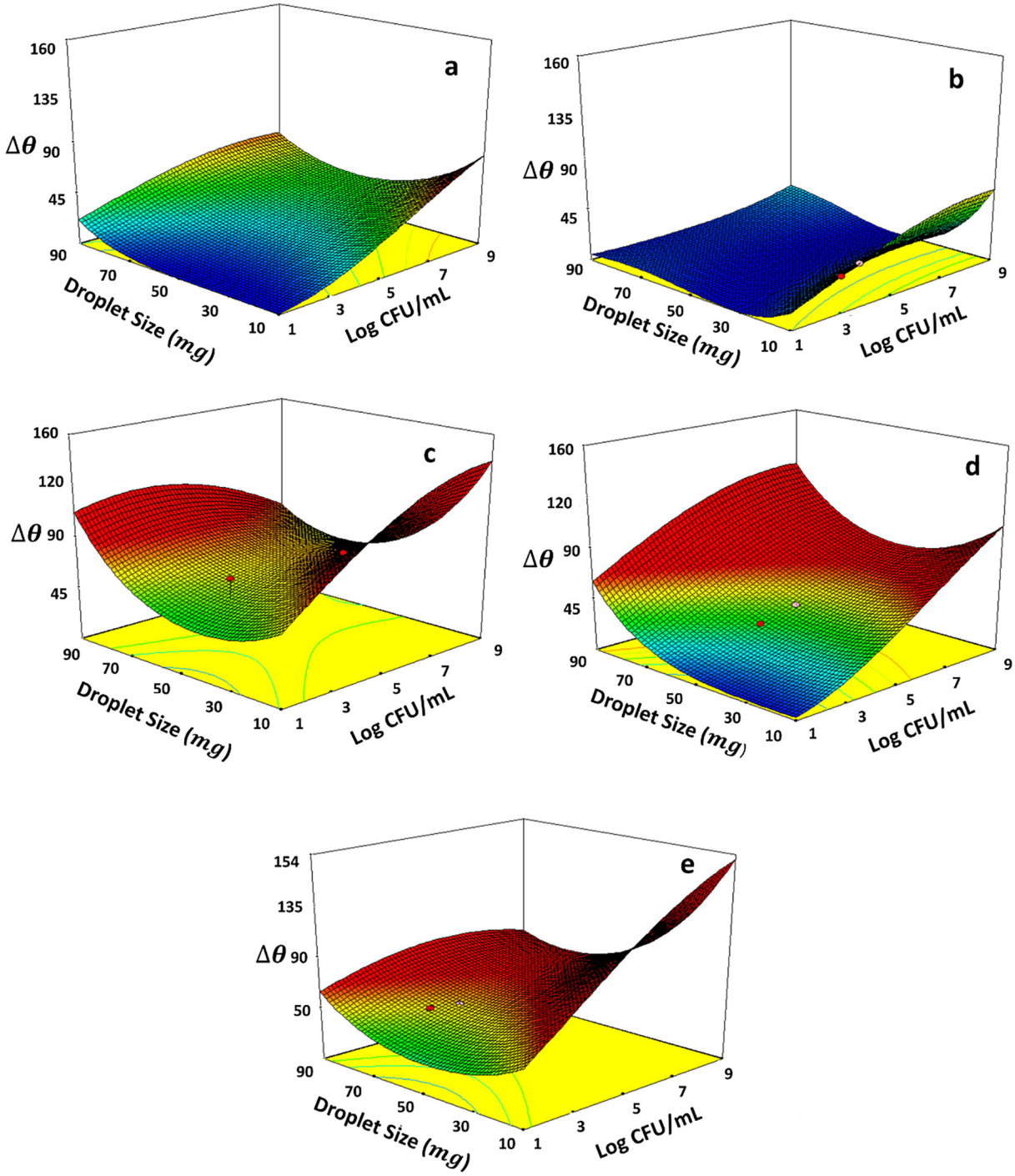

Fig. 4. Absolute angle (Δθ) as a function of bacterial population and droplet volume on the helical tetragonal solid substrate. a) *L. acidophilus*, b) *S. thermophiles*, c) *L. casei*, d) *L. plantarum*, e) *L. bulgaricus*.

3.6. Optimization of influential parameters on (Δθ)

Design Experts Code was used to optimize the most important variables (i.e. bacterial concentration, droplet size, strain and shape of the substrate) for measuring absolute angle (Δθ) for different bacterial suspensions. The criteria of optimization are set to achieve the highest (Δθ). Optimized results were obtained for superhydrophobic (rose-petal effect) surface and 10 mg droplet size of *L. bulgaricus*, *L. casei*, *L. plantarum*, *L. acidophilus*, and *S. thermophiles*, respectively. The condition for acceptable results in the Design Expert Code was set to desirability values higher than 0.75.

3.7. Application of the method on probiotic bacteria in fermented milk

In Figs. 6 and 7, the cell count of probiotic culture *L. Casei* and *L. plantarum* during fermentation at 32 °C for 24 h are shown, respectively. The bacterial growth was not detected in control treatment without any inoculated probiotics. The cell count population of *L. Casei* and *L. plantarum* in probiotic milk after 24 h fermentation increased to 5.79 ± 0.12 $\log_{10}$ cycles and 4.40 ± 0.14 $\log_{10}$ cycles, respectively. These figures also show the contact angle of a fermented milk droplet on the superhydrophobic (rose-petal effect) surface as a function of time. The contact angle decreased with increasing the bacterial

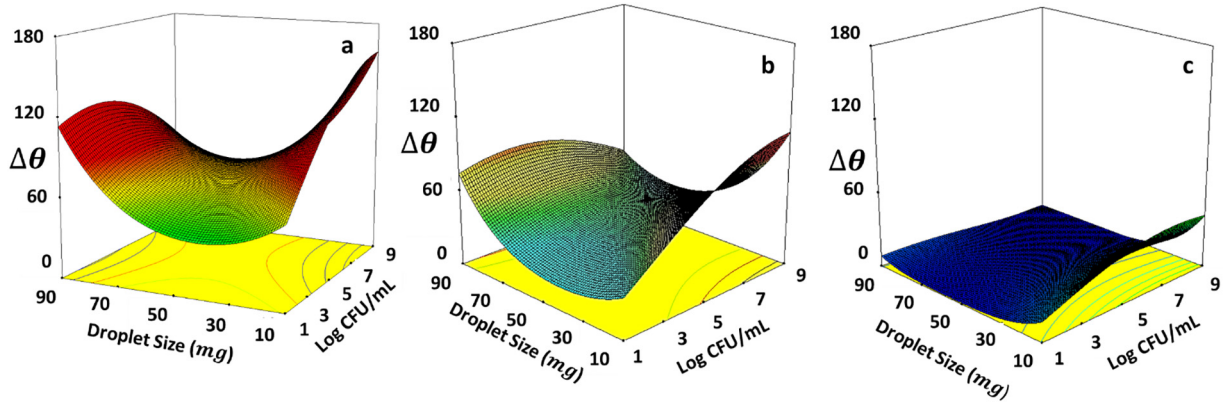

Fig. 5. Absolute angle (Δθ) for *L. casei* as a function of bacterial population and droplet volume on the solid substrate. a) Helical tetragonal, b) L-shaped, c) Nano-rod.

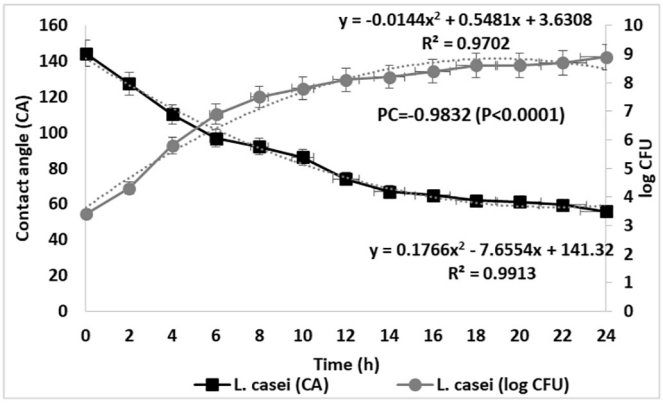

Fig. 6. Contact angles and *L. casei* cell concentration in the probiotic during milk fermentation at 32 °C for 24 h. ■) experimental contact angle; ●) experimental cell concentration. Dashed lines) quadratic regression fitting; PC) Pearson correlation coefficient. The CA are measured on a superhydrophobic ("rose petal-like") surface.

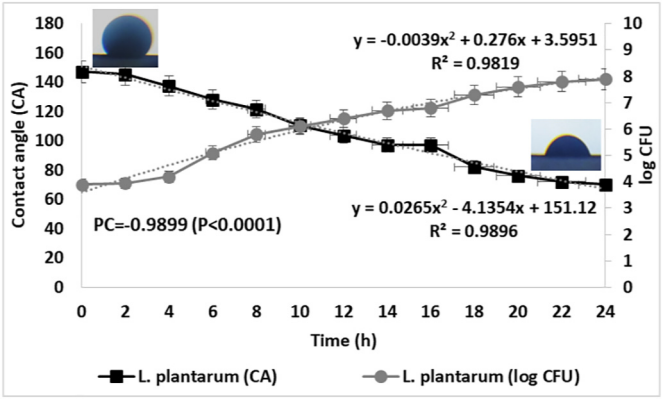

Fig. 7. Contact angles and *L. plantarum* cell concentration in the probiotic during milk fermentation at 32 °C for 24 h. ■) experimental contact angle; ●) experimental cell concentration. Dashed lines) quadratic regression fitting; PC) Pearson correlation coefficient. The CA are measured on a superhydrophobic ("rose petal-like") surface.

concentration in milk. As shown in Figs. 6 and 7, a quadratic equation produces the best fit to the growth and contact angle curves of both probiotic species in fermented milk.

The results of analysis of the cell count of probiotic culture and the contact angle of a fermented milk droplet on the superhydrophobic (rose-petal effect) surface showed very high correlation, with Pearson correlation coefficients −0.9832 ($P < 0.0001$) and − 0.9998 ($P < 0.0001$) for *L. Casei* and *L. plantarum* respectively.

The higher reduction of the contact angle of *L. casei*-fermented milk during incubation compared to *L. plantarum* could be due to higher growth rate of *L. Casei* species. The minimum recommended level of viable probiotic cells at the time of consumption is approximately 10^6 CFU/mL (Adhikari et al., 2003). Therefore, according to the results obtained in this study, it can be said that the bacterial concentration can be quickly estimated by using a droplet of liquid containing probiotics and a superhydrophobic (rose-petal effect) surface. In addition, this method can be applied in other diluted liquid foods (drinks, yogurt, and fruit juices) and for other hydrophobic species.

4. Conclusion

A method is proposed for fast estimation of dairy lactic acid bacterial concentration (diluted liquids) using the hydrophobic surface property of these bacteria together with the superhydrophobic (rose-petal effect) solid surfaces. The method is based on the changes observed for surface free energy and liquid behavior at the interfacial area with the superhydrophobic (rose-petal effect) surface. Three different surface morphologies (sculptured thin films) were designed and fabricated, namely nano-rod, helical tetragonal and L-shaped for this purpose. The values of contact angle and zeta potential were obtained for dried surfaces of 5 conventional dairy bacterial strains. Investigations on the conventional strains used in the dairy industry showed that most of these strains have hydrophobic surfaces and when dispersed in a liquid medium, strongly affect the solid-liquid and liquid-vapor surface tensions, which are dependent on the bacterial concentration. Response surface methodology (RSM) results showed that the type of strain, number of bacteria, drop volume and morphology of the solid surface have significant effect on the surface wettability. It is shown the contact angle of the suspension droplet (e.g., probiotic-fermented milk) change by the type and concentration of bacteria. Therefore, the proposed method can be a viable, easy to perform and economical technique for rapid estimation of bacterial concentration.

Declaration of Competing Interest

The authors declare no competing interest.

Acknowledgments

This work was carried out with the support of the University of Tehran and the Islamic Azad University. The method described in this work is patented by the Iranian authorities under patent number: 139650140003002593 and international number: G01N 30/00.

References

Adhikari, K., Mustapha, A., Grün, I.U., 2003. Survival and metabolic activity of microencapsulated *Bifidobacterium longum* in stirred yogurt. J. Food Sci. 68, 275–280.

Bellon-Fontaine, M.N., Rault, j., Van Oss, C.J., 1996. Microbial adhesion to solvents: a novel method to determine the electron-donor/electron-acceptor or Lewis acid-base properties of microbial cells. Colloids Surf. B 7, 47–53.

Bohinc, K., Dražić, G., Abram, A., Jevšnik, M., Jeršek, B., Nipič, D., Kurinčič, M., Raspor, P., 2016. Metal surface characteristics dictate bacterial adhesion capacity. Int. J. Adhes. Adhes. 68, 39–46.

Boonaert, C.J.P., Rouxhet, P., 2000. Surface of lactic acid bacteria: relationships between chemical composition and physicochemical properties. Appl. Environ. Microbiol. (6), 2548–2554.

Cuperus, P.L., Van der Mei, H.C., Reid, G., Bruce, A.W., Khoury, A.H., Rouxhet, P.G., Busscher, H.J., 1993. Physicochemical surface characteristics of urogenital and poultry lactobacilli. J. Colloid Interface Sci. 156, 319–332.

Deepika, G., Charalampopoulos, D., 2010. Chapter 4 – surface and adhesion properties of lactobacilli. Adv. Appl. Microbiol. 70, 127–152.

Di Ciccio, P., Vergara, A., Festino, A.R., Paludi, D., Zanardi, E., Ghidini, S., Ianieri, A., 2015. Biofilm formation by Staphylococcus aureus on food contact surfaces: relationship with temperature and cell surface hydrophobicity. Food Control 50, 930–936.

Fernandes, P.É., São José, J.F.B., Zerdas, E.R.M.A., Andrade, N.J., Fernandes, C.M., Silva, L.D., 2014. Influence of the hydrophobicity and surface roughness of mangoes and tomatoes on the adhesion of *Salmonella enterica* serovar *Typhimurium* and evaluation of cleaning procedures using surfactin. Food Control 41, 21–26.

Frece, J., Kos, B., Svetec, I.K., Zgaga, Z., Mrsa, V., Suskovic, J., 2005. Importance of S-layer proteins in probiotic activity of *Lactobacillus acidophilus* M92. J. Appl. Microbiol. 98, 285–292.

Gao, L., McCarthy, T.J., Zhang, X., 2009. Wetting and Superhydrophobicity. Langmuir 25 (24), 14100–14104.

Hosseini, S., Savalon, H., Shahraki, M.G., 2017. Design and engineering of sculptured nano-structures for application in hydrophobicity. Ind. Eng. Chem. Res. 45, 391–403.

Kwok, Y., Neumann, A.W., 1999. Contact angle measurement and contact angle interpretation. Adv. Colloid Interf. Sci. 81, 167–173.

Kwon, H.M., Paxson, A.T., Varanasi, K.K., Patankar, N.A., 2011. Rapid deceleration-driven wetting transition during pendant drop deposition on superhydrophobic surfaces. Phys. Rev. Lett. 106, 3–21.

Macciola, V., Candela, G., De Leonardis, A., 2008. Rapid gas-chromatographic method for the determination of diacetyl in milk, fermented milk and butter. Food Control 19, 873–878.

Mazumdara, S.D., Hartmann, M., Kuampfer, P., Keusgen Nakhondam, M., 2007. Rapid method for detection of Salmonella in milk by surface plasmon resonance (SPR). Biosens. Bioelectron. 22, 2040–2046.

Mozes, N., Handley, P.S., Busscher, H.J., Rouxhet, P.G., 1991. Microbial Cell Surface Analysis: Structural and Physicochemical Methods. VCH Publishers, Inc., New York.

Murakami, D., Jinnai, H., Takahara, A., 2014. Wetting transition from the cassie–baxter state to the wenzel state on textured polymer surfaces. Langmuir 30, 2061–2067.

Neu, T.R., 1996. Significance of bacterial surface-active compounds in interaction of bacteria with interfaces. Microbiol. Rev. 60, 151–166.

Pelletier, C., Bouley, C., Cayuela, C., Bouttier, S., Bourlioux, P., Bellon-Fontaine, M.N., 1997. Cell surface characteristics of *Lactobacillus casei* subsp *casei*, *Lactobacillus paracasei* subsp *paracasei*, and *Lactobacillus rhamnosus* strains. Appl. Environ. Microbiol. 63, 1725–1731.

Pretzer, G., Snel, J., Molenaar, D., Wiersma, A., Bron, P.A., Lambert, J., de Vos, W.M., van der Meer, R., Smits, M.A., Kleerebezem, M., 2005. Biodiversity-based identifi-cation and functional characterization of the mannose-specific adhesion of *Lactobacillus plantarum*. J. Bacteriol. 187, 6128–6136.

Reid, G., Cuperus, P.L., Bruce, A.W., Vander Mei, E., Tomeczek, L., Khoury, A.H., Busscher, H.J., 1992. Comparison of contact angles and adhesion to hexadecane of urogenital, dairy, and poultry lactobacilli: effect of serial culture passages. Appl. Environ. Microbiol. 2, 1549–1553.

Rijnaarts, H.H.M., Norde, W., Bouwer, E.J., Lyklema, J., Zehnder, A.J.B., 1995. Reversibility and mechanism of bacterial adhesion. Colloids Surf. B 4, 5–22.

Shobharani, P., Agrawal, R., 2010. Interception of quorum sensing signal molecule by furanone to enhance shelf life of fermented milk. Food Control 21, 61–69.

Stalder, A.F., Kulik, G., Sage, D., Barbieri, L., Hoffmann, P., 2006. A snake based approach to accurate determination of both contact points and contact angles. Colloids Surf. A Physicochem. Eng. Asp. 286, 92–103.

Stanton, M.M., Ducker, R.E., MacDonald, J.C., Lambert, C.R., McGimpsey, W.G., 2012. Super-hydrophobic, highly adhesive, polydimethylsiloxane (PDMS) surfaces. J. Colloid Interface Sci. 367, 502–508.

Tharmaraj, N., Shah, N.P., 2003. Selective enumeration of *Lactobacillus delbrueckii* ssp. *bulgaricus*, *Streptococcus thermophilus*, *Lactobacillus acidophilus*, Bifidobacteria, *Lactobacillus casei*, *Lactobacillus rhamnosus*, and Propionibacteria. J. Dairy Sci. 86, 2288–2296.

Tymczyszyn, E.E., Díaz, R., Pataro, A., Sandonato, N., Gómez-Zavaglia, A., Disalvo, E.A., 2008. Critical water activity for the preservation of Lactobacillus bulgaricus by vacuum drying. Int. J. Food Microbiol. 128, 342–347.

Välimaa, A.L., Tilsala-Timisjärvi, A., Virtanen, E., 2015. Rapid detection and identification methods for listeria monocytogenes in the food chain – a review. Food Control 55, 103–114.

Van Oss, C.J., 2006. Interfacial Force in Aqueous Media. Taylor & Francis Publishing, New York.

Van Oss, C.J., Good, R.J., Chaudhury, M.K., 1986. The role of van der Waals forces and hydrogen bonds in “hydrophobic interactions” between biopolymers and low energy surfaces. J. Colloid Interface Sci. 111, 378–390.

Yang, C., Tartaglino, U., Persson, B.N.J., 2006. Influence of surface roughness on Superhydrophobicity. Phys. Rev. Lett. 97, 116103(1)–4.

Young, T., 1805. An essay on the cohesion of fluids. Philos. Trans. R. Soc. Lond. 95, 65–87.